

Southern Ocean removing carbon dioxide from atmosphere more efficiently

Scientists compile densest carbon data set in Antarctic waters

Source: AWI

Since 2002, the Southern Ocean has been removing more of the greenhouse gas carbon dioxide from the atmosphere, according to two new studies.

These studies make use of millions of ship-based observations and a variety of data analysis techniques to conclude that the Southern Ocean has increasingly taken up more carbon dioxide during the last 13 years. That follows a decade from the early 1990s to 2000s, where evidence suggested the Southern Ocean carbon dioxide sink was weakening. The new study appear in the American Geophysical Union journal *Geophysical Research Letters*.

The global oceans are an important sink for human-released carbon dioxide, absorbing nearly a quarter of the total carbon dioxide emissions every year. Of all ocean regions, the Southern Ocean below the 35th parallel south plays a particularly vital role. Although it comprises only 26% of the total ocean area, the Southern Ocean has absorbed nearly 40 percent of all anthropogenic carbon dioxide taken up by the global oceans up to the present, says David Munro, a scientist at the Institute of Arctic and Alpine Research (INSTAAR) at the University of Colorado Boulder, and an author on the GRL paper.

The GRL paper focuses on one region of the Southern Ocean extending from the tip of South America to the tip of the Antarctic Peninsula. The Drake Passage is the windiest, roughest part of the Southern Ocean. The critical element to this study is that we were able to sustain measurements in this harsh environment as long as we have--both in the summer and the winter, in every year over the last 13 years. This data set of ocean carbon measurements is the densest ongoing time series in the Southern Ocean.

The team was able to take these long-term measurements by piggybacking instruments on the Antarctic Research Supply Vessel Laurence M. Gould. The National Science Foundation-supported Gould, which makes nearly 20 crossings of the Drake Passage each year, transporting people and supplies to and from Antarctic research stations. For over 13 years, it's taken chemical measurements of the atmosphere and surface ocean along the way.

By analyzing more than one million surface ocean observations, the researchers could tease out subtle differences between the carbon dioxide trends in the surface ocean and the atmosphere that suggest a strengthening of the carbon sink. This change is most pronounced in the southern half of the Drake Passage during winter. Although the researchers aren't sure of the exact mechanism driving these changes, "it's likely that winter mixing with deep waters that have not had contact with the atmosphere for several hundred years plays an important role," says Munro.

The Science paper, led by Peter Landschützer at the ETH Zurich, takes a more expansive view of the Southern Ocean. This study uses two innovative methods to analyze a dataset of surface water carbon dioxide spanning almost three decades and covering all of the waters below the 35th parallel south. These data—including Sweeney and Munro's data from the Drake Passage—also show that the surface water carbon dioxide is increasing slower than atmospheric carbon dioxide, a sign that the Southern Ocean as a whole is more efficiently removing carbon from the atmosphere. These results contrast with previous findings that showed that the Southern Ocean carbon dioxide sink was stagnant or weakening from the early 1990s to the early 2000s.

In addition to the Drake Passage measurements, the Science paper uses datasets that represent a significant international collaboration, including carbon dioxide sampling from NOAA's Ship of Opportunity Program. This program, led by Rik Wanninkhof of NOAA's Atlantic Oceanographic and Meteorological Laboratory (AOML) who is also a co-author of the Science paper, is the world's largest coordinated carbon dioxide sampling operation. Despite all these efforts, the Southern Ocean remains under-sampled. Given the importance of the Southern Ocean to the global oceans' role in absorbing atmospheric carbon dioxide, these studies suggest that density of measurements must continue to increase in this part of the world despite the challenging environment.

The GRL reprint follows

Title

Recent evidence for a strengthening CO₂ sink in the Southern Ocean from carbonate system measurements in the Drake Passage (2002-2015)

Authors

David R. Munro

Department of Atmospheric and Oceanic Sciences and Institute of Arctic and Alpine Research, University of Colorado, Boulder, CO, USA

Nicole S. Lovenduski

Department of Atmospheric and Oceanic Sciences and Institute of Arctic and Alpine Research, University of Colorado, Boulder, CO, USA

Taro Takahashi

Lamont-Doherty Earth Observatory, Columbia University, Palisades, NY, USA

Britton B. Stephens

National Center for Atmospheric Research, Boulder, CO, USA

Timothy Newberger

Cooperative Institute for Research in Environmental Sciences, University of Colorado, Boulder, CO, USA

Colm Sweeney

Cooperative Institute for Research in Environmental Sciences, University of Colorado, Boulder, CO, USA

Key Points

- Ocean pCO₂ increasing more slowly than atmospheric pCO₂ south of the Antarctic Polar Front
- Lack of winter TCO₂ increase and cooling summer sea surface temperatures drive ocean pCO₂ trends
- Lack of winter TCO₂ increase causes temporary winter stability in carbonate ion concentration

This article has been accepted for publication and undergone full peer review but has not been through the copyediting, typesetting, pagination and proofreading process which may lead to differences between this version and the Version of Record. Please cite this article as doi: 10.1002/2015GL065194

Abstract

We present a 13-year (2002-2015) semi-monthly time-series of the partial pressure of CO₂ in surface water (pCO_{2surf}) and other carbonate system parameters from the Drake Passage. This record shows a clear increase in the magnitude of the sea-air pCO₂ gradient, indicating strengthening of the CO₂ sink in agreement with recent large-scale analyses of the world oceans. The rate of increase in pCO_{2surf} north of the Antarctic Polar Front (APF) is similar to the atmospheric pCO₂ (pCO_{2atm}) trend, whereas the pCO_{2surf} increase south of the APF is slower than the pCO_{2atm} trend. The high-frequency surface observations indicate that an absence of a winter increase in total CO₂ (TCO₂) and cooling summer sea surface temperatures are largely responsible for increasing CO₂ uptake south of the APF. Muted winter trends in surface TCO₂ also provide temporary stability to the carbonate system that is already close to undersaturation with respect to aragonite.

Introduction

Approximately 40 % of the oceanic inventory of anthropogenic CO₂ has entered south of 40°S (Khaliwala et al., 2009). Studies based on observations and climate models have indicated that changes in ocean circulation associated with climate variability may have reduced the efficiency of uptake of CO₂ in the Southern Ocean over the past few decades (Le Quéré et al., 2010; Metzl, 2009; Lovenduski et al., 2013). In contrast, recent studies by Landschützer et al. (2014) and Majkut et al. (2014) suggest that global ocean uptake of CO₂ has increased over the past decade due in large part to the Southern Ocean. These studies included significant contributions of data from the Drake Passage Time-series (DPT) (Landschützer et al. (2014) and Majkut et al. (2014) include DPT data through 2011 and 2009, respectively), but the impact of the DPT observations is obscured by data-assimilation or neural network schemes required to make basin-scale estimates of interannual variability. Similarly, Fay et al. (2014) analyzed multiple pCO_{2,surf} records, including DPT data through 2010, and report a strengthening Southern Ocean CO₂ sink since 2007. These studies suggest that some combination of trends in sea surface temperature (SST) and the Southern Annular Mode (SAM) may be responsible for the recent observed increase in Southern Ocean CO₂ uptake. Here we show using a single highly resolved time-series that the increase in CO₂ uptake in Drake Passage south of the Antarctic Polar Front (APF) is driven by the combination of near-zero time trends in winter TCO₂ and declines in summer SST.

The air-sea CO₂ flux is difficult to observe directly and depends on both chemical (i.e., the disequilibrium of CO₂ between surface ocean and atmosphere) and physical (i.e., wind) forcing. The physical forcing is typically estimated using a parameterization of the dependence of gas exchange on wind speed (e.g., Sweeney et al., 2007) and the chemical forcing by the difference between the partial pressures of CO₂ in the surface ocean (pCO_{2surf}) and atmosphere (pCO_{2atm}) commonly referred to as the ΔpCO₂. Since uncertainty in the gas exchange parameterization and variability in wind speeds obscures long-term trends in the air-sea CO₂ flux, several recent investigations of CO₂ uptake focus on trends in ΔpCO₂ (e.g., Lovenduski et al., 2015; Fay et al., 2014) or the trend in pCO_{2surf} relative to the trend in atmospheric CO₂ (e.g., Lenton et al., 2012, Takahashi et al., 2012; Metzl et al., 2009) and neglect the influence of variability and long-term trends in wind speed on air-sea CO₂ flux due to variability and trends in the gas transfer velocity.

Oceanic uptake of CO₂ also leads to acidification, which is characterized by decreases in the surface ocean pH, carbonate ion concentration ([CO₃²⁻]), and the saturation states of the calcium carbonate minerals aragonite (Ω_{arag}) and calcite (Ω_{calc}). The Southern Ocean is particularly vulnerable to the effects of ocean acidification due to its naturally low surface [CO₃²⁻] (Fabry et al., 2009). McNeil and Matear (2008) suggested that the Southern Ocean could become seasonally undersaturated with respect to aragonite within the next several decades. Several recent papers have examined long-term trends of pCO_{2surf}, pH, [CO₃²⁻], Ω_{arag}, and Ω_{calc} at ocean time-series sites (e.g., Bates

et al., 2014; Takahashi et al., 2014) and documented significant decreases in pH, $[\text{CO}_3^{2-}]$, Ω_{arag} , and Ω_{calc} over the past several decades associated with an increase in $\text{pCO}_{2\text{surf}}$.

Ocean time-series are necessarily concentrated in the Northern Hemisphere and observations in the Southern Hemisphere are particularly sparse during the winter when wind speeds and air-sea exchange rates of CO_2 are presumably greatest. This data gap represents a source of significant uncertainty to current understanding of the global ocean CO_2 flux (Landschützer et al., 2014).

In response to this data gap and the growing awareness of the importance of the Southern Ocean in the global climate system and carbon cycle, $\text{pCO}_{2\text{surf}}$ and carbonate system observations within mid and high-latitude Southern Hemisphere waters have increased markedly over the past decade, including a new time-series in the sub-Antarctic zone (SAZ) south of Australia (Shadwick et al., 2015) and intensified sampling in regions close to the Antarctic continent (Mattsdotter Björk et al., 2014; Roden et al., 2013; Shadwick et al., 2013; van Heuven et al., 2013; Hauck et al., 2010). Initiated in 2002 and continuing to present, the DPT is unique among Southern Ocean research programs in both its spatial and temporal coverage. Spatially, the DPT spans the Antarctic Circumpolar Current (ACC) region including both the Antarctic Zone (AZ) south of the APF and the Polar Frontal Zone (PFZ) between the APF and Sub-Antarctic Fronts (SAF). Temporally, underway observations of $\text{pCO}_{2\text{surf}}$ and atmospheric CO_2 are made on nearly 20 crossings per year; discrete observations of total CO_2 (TCO_2), the isotopic composition of TCO_2 (both T^{13}CO_2 and T^{14}CO_2), inorganic macronutrient concentrations

(including NO_3^- , PO_4^{3-} , and $\text{Si}(\text{OH})_4$), and salinity are collected at every half degree of latitude on 5 to 8 crossings per year. DPT is notable for sampling during the austral winter (see Fig. 2b of Wanninkhof et al., 2013) in all years from 2002 to present. DPT is also notable because trends identified across the Drake Passage are likely to stretch into the middle of the Pacific sector of the Southern Ocean. This was demonstrated by a correlation analysis of satellite SST and chlorophyll observations (i.e., two parameters strongly linked to air-sea CO_2 fluxes) between Drake Passage and the rest of the Southern Ocean showing that trends in Drake Passage are representative of trends in the ACC region as far as 1200 km west of the Drake Passage (Munro et al., 2015).

The $\text{pCO}_{2\text{surf}}$ observations from the DPT have become the backbone of larger datasets used to examine trends and estimate CO_2 uptake for the broader Southern Ocean (e.g., Fay et al., 2014; Landschützer et al., 2014; Majkut et al., 2014; Lenton et al., 2013; Wanninkhof et al., 2013; Lenton et al., 2012). However, all of these studies have relied on significant averaging or interpolation using parameters such as satellite observations of SST or chlorophyll and climatologies of mixed layer depth to make basin-scale estimates of trends. These methodologies potentially induce or hide actual trends due to sampling biases or exaggerated dependences of trends on other variables. This study uses the high-frequency observations made in the Drake Passage to directly estimate and better understand where (relative to the APF) and when (seasonality) trends in the carbonate system are most pronounced. We utilize the full set of underway $\text{pCO}_{2\text{surf}}$ observations combined with discrete TCO_2 , salinity and nutrient measurements to

estimate seawater carbonate system parameters including pH, $[\text{CO}_3^{2-}]$, Ω_{arag} , and Ω_{calc} at the same temporal resolution as underway $\text{pCO}_{2\text{surf}}$. We then analyze and discuss trends in carbonate parameters from this high-resolution Southern Ocean record for the years 2002-2015. This analysis expands on a previous study by Takahashi et al. (2014) who presented an analysis of DPT data based on the sparsely-sampled discrete TCO_2 samples and the associated subset of underway $\text{pCO}_{2\text{surf}}$ observations. This analysis takes advantage of the high-resolution $\text{pCO}_{2\text{surf}}$ data to significantly reduce the uncertainty in seasonal trends.

Methods

Analytical methods used to measure pCO_2 , TCO_2 and nutrients as well as the methods used to calculate carbonate parameters are described in detail in Munro et al. (2015). All measurements were averaged spatially into the four regions (Fig. 1) used by Munro et al. (2015) and temporally by month. The four regions in Fig. 1 are oriented parallel to the mean flow of the ACC such that two regions are located north (i.e., Regions 1 and 2) and south (i.e., Regions 3 and 4) of the APF. The boundaries of these regions exclude coastal waters and higher productivity waters northeast of the Antarctic Peninsula.

The mole fraction of CO₂ was measured from air equilibrated with surface water ($x\text{CO}_{2\text{surf}}$) and the atmosphere ($x\text{CO}_{2\text{atm}}$) aboard the Antarctic Research Supply Vessel (ARSV) *Laurence M. Gould*. The $x\text{CO}_{2\text{atm}}$ observations were filtered to exclude times of stack air contamination based on short term CO₂ variability and agree with NOAA Greenhouse Gas Reference Network flask and the associated NOAA Earth System Research Laboratory Greenhouse Gas Marine Boundary Layer (MBL) Reference (<http://www.esrl.noaa.gov/gmd/ccgg/mbl/index.html>) to better than 0.2 $\mu\text{mol CO}_2$ per mole of dry air (the DPT atmospheric measurements reported here were not used to create the MBL reference). Despite the close agreement, we used the MBL Reference for $x\text{CO}_{2\text{atm}}$ values in all available years (i.e., 2002-2013) because too few DPT atmospheric measurements were made during the first 8 months of the record to filter out stack gas contamination. The $p\text{CO}_{2\text{atm}}$ and $p\text{CO}_{2\text{surf}}$ were calculated from MBL $x\text{CO}_{2\text{atm}}$ and $x\text{CO}_{2\text{surf}}$, respectively, using ship observations of atmospheric pressure and assuming 100 % water vapor saturation. The analytical precision of $p\text{CO}_{2\text{surf}}$ values is estimated to be better than 1.5 μatm . The $\Delta p\text{CO}_2$ ($p\text{CO}_{2\text{surf}} - p\text{CO}_{2\text{atm}}$) was calculated at the location of each $p\text{CO}_{2\text{surf}}$ value (2.5 minute sampling interval). In this analysis, a positive (negative) $\Delta p\text{CO}_2$ indicates a flux of CO₂ out of (into) the ocean.

Analytical precision for TCO₂ observations was estimated at $\pm 1 \mu\text{mol kg}^{-1}$ (Chipman et al., 1993). Total alkalinity (TA) was calculated from TCO₂, $p\text{CO}_{2\text{surf}}$, PO_4^{3-} , and Si(OH)_4 observations at each location where discrete samples were collected using the dissociation constants of Lueker et al. (2000) for carbonic acid. The estimated

accuracy of each TA value based on the analytical precisions for TCO_2 and $\text{pCO}_{2\text{surf}}$ measurements given above is $\pm 2 \mu\text{eq kg}^{-1}$. The computed TA values have been shown to be consistent with values measured by titration (Takahashi et al., 2014). Multiple linear regressions were used to model TA as a function of temperature and salinity for each region based on discrete observations. TA was estimated at the spatial and temporal resolution of underway observations using regional relationships and underway temperature and salinity measurements. Estimated TA and $\text{pCO}_{2\text{surf}}$ observations were then used to calculate additional carbonate parameters (i.e., TCO_2 , pH, $[\text{CO}_3^{2-}]$, Ω_{arag} , and Ω_{calc}). Comparison of TA values calculated with regional temperature-salinity-TA relationships and discrete TA values yields root-mean-square deviations of 5, 5, 6, and 5 $\mu\text{eq kg}^{-1}$ for Regions 1 through 4, respectively.

All trends were calculated using a linear least-squares approach after removing seasonal variability using monthly time-series means similar to Bates et al. (2014). Confidence intervals in all trends are given by the 1σ standard error of the slope similar to Bates et al. (2014), Fay et al. (2014), and Fay and McKinley (2013). Two trends are assumed to be statistically different from one another or zero if the 1σ confidence intervals fail to overlap following the approach of Fay et al. (2014) and Fay and McKinley (2013).

Variability in $\text{pCO}_{2\text{surf}}$, pH, $[\text{CO}_3^{2-}]$, Ω_{arag} , and Ω_{calc} can be expressed as the sum of changes due to variability in SST, sea surface salinity (SSS), TA, and TCO_2 (e.g., Takahashi et al., 2014; Lenton et al., 2012; Takahashi et al., 1993). Here we use the

equations presented in Takahashi et al. (2014) who evaluated the effects of temperature, salinity, TA, and TCO₂ on the observed seasonal change in pCO_{2surf}, pH, Ω_{arag}, and Ω_{calc} for Drake Passage and other ocean time-series. The small differences between the summation of the four pCO_{2surf} drivers (i.e., temperature, salinity, TA, and TCO₂) and observed pCO_{2surf} trends in this study can be attributed the use of a single value for the CO₂ and TA Revelle factors and to the approximation of the change in pCO_{2surf}, pH, Ω_{arag}, and Ω_{calc} with each of the four drivers (Takahashi et al., 2014; Lenton et al., 2012; Takahashi et al., 1993). Additionally, salinity changes influence both TA and TCO₂ and the effect of salinity trends on these two drivers can be separated into salinity-normalized and salinity-driven components following Lovenduski et al. (2007). We use the approach of Lovenduski et al. (2007) to separate the influence of salinity trends on TCO₂-driven trends for pCO_{2surf}, pH, Ω_{arag}, and Ω_{calc}.

Results and Discussion

Our measurements in the Drake Passage reveal that overall the region is a weak sink of CO₂, because pCO_{2atm} is on average greater than pCO_{2surf} (Drake Passage ΔpCO₂ = -2.37 ± 0.04 μatm based on an unweighted mean ± 1σ standard error of all measurements within Regions 1-4). Fig. 2a shows that the weak CO₂ sink in the Drake Passage represents a balance between a near neutral region north of the APF (unweighted

mean $\pm 1\sigma$ standard error of all $\Delta p\text{CO}_2$ observations in Regions 1 and 2 = $+0.26 \pm 0.05$ μatm) and a sink region south of the APF (unweighted mean $\pm 1\sigma$ standard error of all $\Delta p\text{CO}_2$ observations in Regions 3 and 4 = -4.77 ± 0.05 μatm).

The time-series $p\text{CO}_{2\text{surf}}$ trend of 1.52 ± 0.15 $\mu\text{atm yr}^{-1}$ (Table S1a) for the Drake Passage (i.e., all four regions in Fig. 1) is significantly lower than the $p\text{CO}_{2\text{atm}}$ trend (1.77 ± 0.08 $\mu\text{atm yr}^{-1}$). The magnitude of the $p\text{CO}_{2\text{surf}}$ trend decreases from north to south across Drake Passage (Table S1a) with trends for Regions 1 and 2 (1.74 ± 0.15 and 1.70 ± 0.15 $\mu\text{atm yr}^{-1}$, respectively) close to the trend in $p\text{CO}_{2\text{atm}}$ and trends for Regions 3 and 4 (1.34 ± 0.19 and 1.16 ± 0.27 $\mu\text{atm yr}^{-1}$, respectively) significantly below the $p\text{CO}_{2\text{atm}}$ trend. This means that $\Delta p\text{CO}_2$ becomes more negative with time in Regions 3 and 4 (Tables 1 and S1a), indicating a strengthening CO_2 sink south of the APF over the time-series. Trends for pH, $[\text{CO}_3^{2-}]$, Ω_{arag} , and Ω_{calc} show declines over the time-series and decrease in magnitude from north to south across Drake Passage consistent with $p\text{CO}_{2\text{surf}}$ (Table S1a), although the values overlap within the estimated uncertainties.

An analysis of Drake Passage trends in $p\text{CO}_{2\text{surf}}$, pH, $[\text{CO}_3^{2-}]$, Ω_{arag} , and Ω_{calc} for austral summer (i.e., December, January, and February) and winter (i.e., July, August, and September) yields slower rates of change in winter (Figs. 2d and 2e; Tables 1, S2a and S2b) particularly south of the APF. Consequently, the seasonal amplitude in $p\text{CO}_{2\text{surf}}$ and most other carbonate parameters decreases significantly south of the APF over the time-series (Fig. S1; Table S3). As a result of the small wintertime $p\text{CO}_{2\text{surf}}$ trends observed (in Regions 3 and 4) south of APF, the $\Delta p\text{CO}_2$ becomes increasingly negative

and this trend is greatest in winter (Fig. 2c; Table 1). Despite the low number of crossings during the austral winter relative to the total number of crossings, trends can be calculated with similar confidence intervals to annual trends (Tables 1, S1a and S2b) due to low wintertime variability (Figs. 2a-e). In contrast, uncertainties in summer trends (Tables 1 and S2a) are greater as a result of physical and biological variability (e.g., spatiotemporal variability in biological CO₂ uptake and mixed layer depth).

Analysis of the drivers of observed trends in pCO_{2surf}, pH, Ω_{arag} , and Ω_{calc} (Fig. 3; Table S4) for all months indicate that observed trends in pCO_{2surf} and pH are primarily a function of increases in TCO₂ and decreases in SST over the time-series. However, we find significant differences between drivers of observed trends in summer and winter (Fig. 3; Table S4). In summer, pCO_{2surf} and pH trends in all regions are primarily caused by large increases in TCO₂ that are partially offset by decreases in SST (Fig. 3; Tables S2 and S4). Normalization of TCO₂ to a constant salinity (sTCO₂) (Fig. 3; Table S4) suggests that a summer increase in salinity (Table S2) accounts for approximately one fourth of the TCO₂-driven component of the pCO_{2surf} trends (Fig. 3; Table S4).

In contrast, the winter TCO₂-driven pCO_{2surf} trends are absent throughout Drake Passage (Fig. 3; Table S4). Although there is a small winter decrease in salinity (Table S2) that contributes modestly to observed trends (Fig. 3; Table S4), this change is insufficient to explain the small winter trends in TCO₂ and pCO_{2surf} south of the APF (Table S2). We suggest that winter surface waters south of the APF are less affected by the rise in atmospheric CO₂ relative to waters further north because it is here that large

reservoirs of deep water with low anthropogenic CO₂ (Pardo et al., 2014) are entrained into surface waters (Takahashi et al., 1997). While cooling surface waters during other seasons (Table S2) contribute to an increasingly negative annual $\Delta p\text{CO}_2$ (e.g., Fay et al., 2014; Majkut et al., 2014), this effect is not apparent during winter in the Drake Passage (Table S2). Additionally, we note a low correlation between variability in the $\Delta p\text{CO}_2$ for Drake Passage and variability of the SAM index ($R^2 = 0.19$ using annual values).

The annual growth rates and drivers of $p\text{CO}_{2\text{surf}}$ can be compared to the analysis of Lenton et al. (2012) who utilized all available $p\text{CO}_{2\text{surf}}$ data for the years 2001-2008 from 45-62° S and 0-65° W which approximates the Atlantic sector of the Southern Ocean. Observed annual $p\text{CO}_{2\text{surf}}$ trends are lower than the atmospheric trends for both studies indicating growth in ocean CO₂ uptake; however, the annual trend reported by Lenton et al. (2012) ($0.2 \pm 1.0 \mu\text{atm yr}^{-1}$) is significantly smaller than observed in the current study ($1.52 \pm 0.15 \mu\text{atm yr}^{-1}$). Seasonal trends and drivers of observed trends differ more substantially; Lenton et al. (2012) reported negative summer $p\text{CO}_{2\text{surf}}$ trends ($-0.9 \pm 2.5 \mu\text{atm yr}^{-1}$) and positive winter $p\text{CO}_{2\text{surf}}$ trends ($2.2 \pm 1.0 \mu\text{atm yr}^{-1}$) larger than the atmospheric trend and opposite to the current study (Table S2). The negative summer trends in $p\text{CO}_{2\text{surf}}$ reported by Lenton et al. (2012) are linked to large declines in $s\text{TCO}_2$ and contrast with the positive summer $s\text{TCO}_2$ trends observed in the current study. Both studies note a salinity increase in summer although the influence of salinity on TCO_2 in the current study is smaller than observed by Lenton et al. (2012). Differences between these two analyses can be attributed to the different spatial domains (i.e., Lenton et al.

(2012) includes biologically productive regions to the east of Drake Passage) and time intervals (i.e., the current study includes six additional years) represented by the two studies.

To demonstrate the significance of the DPT as an ocean time-series, we compare the trends in DPT $p\text{CO}_{2\text{surf}}$, TCO_2 , pH, and Ω_{arag} to trends reported from seven other long-running open-ocean time-series sites (Bates et al., 2014) in Fig. S2, where each trend and its uncertainty are plotted as a function of the length of the time-series. While the DPT is shorter than most other time-series, trends calculated from DPT data exhibit low uncertainty (Fig. S2), due to the high temporal resolution (i.e., 20 crossings per year) and small seasonal amplitude in SST and $p\text{CO}_{2\text{surf}}$ relative to most other time-series (Takahashi et al., 2014). A recent model-based study by Lovenduski et al. (2015) also suggests that low seasonal and interannual variability within Drake Passage contributes to the low uncertainty of observed carbonate system trends.

The absence of winter increases in TCO_2 south of the APF (Table S2) also has implications for ocean acidification if current trends continue. McNeil and Matear (2008) projected future trends in $[\text{CO}_3^{2-}]$, Ω_{arag} , and Ω_{calc} using the IPCC IS92a scenario and determined that waters south of the APF around the Southern Ocean could reach undersaturation with respect to aragonite as early as the year 2030 assuming the seasonal amplitude of carbonate parameters remains constant. We find a mean seasonal amplitude in $[\text{CO}_3^{2-}]$ of 10-15 $\mu\text{mol kg}^{-1}$ for Drake Passage (Fig. S1; Table S1b) similar to the analysis of McNeil and Matear (2008) with lowest concentrations observed during

winter. The seasonal amplitude of $[\text{CO}_3^{2-}]$ declines significantly from 2002 to 2015 in all four regions of the Drake Passage with the largest decline in amplitude in Region 4 (Fig. S1; Table S3). Although the length of the DPT is short relative to model-based studies (e.g., Hauck et al., 2015) that investigate long-term shifts in carbonate chemistry, the observed decrease in seasonal amplitude in most carbonate parameters in Drake Passage contrasts with a predicted increase in seasonal amplitudes due to a future decrease in buffer capacity (Egleston et al., 2010; Riebesell et al., 2009). Based on linear extrapolation of summer trends for Region 4 (Tables S2b and S4c), the onset of seasonal aragonite undersaturation south of the APF (i.e., Region 4) could be delayed until the year 2050, two decades after the prediction of McNeil and Matear (2008). Decreasing buffer capacity on decadal timescales (Hauck et al., 2015; Egleston et al., 2010; Riebesell et al., 2009) could further delay summer undersaturation with respect to aragonite by increasing the influence of biological CO_2 uptake on the seasonal summer maximum in aragonite saturation state (Fig. S1).

Conclusions

The Drake Passage Time-series (DPT) provides one of the most extensive datasets of underway and discrete observations from the Southern Ocean and is unique in its coverage during the austral winter. In this analysis we present observations of sea-air

gradients of the partial pressure of CO₂ ($\Delta p\text{CO}_2$) and use underway $p\text{CO}_{2\text{surf}}$ and estimates of TA based on discrete observations to estimate pH, $[\text{CO}_3^{2-}]$, Ω_{arag} , and Ω_{calc} for Drake Passage crossings from 2002-2015. Because of the high resolution of this time-series and low variability of the observations, this dataset provides a unique opportunity to examine long-term trends and drivers of observed trends for different seasons with low uncertainties. Overall, the carbonate system trends from 2002 to 2015 (e.g., the $\Delta p\text{CO}_2$ trend for Drake Passage of $-0.37 \pm 0.16 \mu\text{atm yr}^{-1}$) are consistent with other recent studies (Fay et al., 2014; Landschützer et al., 2014; Majkut et al., 2014; Currie et al., 2011) suggesting that the Southern Ocean is playing an ever-increasing role in taking up atmospheric CO₂.

Importantly, this analysis indicates that $\Delta p\text{CO}_2$ trends are most pronounced south of the APF during winter, suggesting that the recent growth of the Southern Ocean CO₂ sink reported in other studies is driven in part by enhanced wintertime uptake south of the APF. As the region south of the APF is characterized by upwelling of waters with low anthropogenic CO₂ content (Pardo et al., 2014) and mixed layer depths are greatest in winter (Stephenson et al., 2012), it is reasonable to assume that enhanced winter uptake is driven by the stability of $p\text{CO}_2$ in the deep waters underlying this region in conjunction with the rapidly rising atmospheric CO₂ as suggested by Takahashi et al. (1997). Furthermore, a comparison of trends at different global, open-ocean time-series sites demonstrates that uncertainty in the observed trends for the DPT is small despite the relative shortness of the dataset due to the high resolution of the time-series and also

because seasonal and interannual variability is low in the Drake Passage relative to other Southern Ocean regions (Lovenduski et al., 2015). Our measurements show that the amplitude of the seasonal cycle in $[\text{CO}_3^{2-}]$ is decreasing with time and suggest that onset of aragonite undersaturation may be delayed by two decades relative to estimates that assume a constant seasonal cycle into the future.

Accepted Article

Acknowledgements

This research was supported by NSF (PLR-1341647, AOAS-0944761, AOAS-066975, and OCE-1155240) and the NOAA Climate Program Office (NA12OAR4310058). T.T. was supported by NOAA grant NA10OAR4320143. The National Center for Atmospheric Research is sponsored by the National Science Foundation. All TCO₂ measurements were made by John G. Goddard of LDEO. We are grateful for the efforts of the marine and science support teams of the ARSV *Laurence M. Gould* particularly Kevin Pedigo, Bruce Felix, and Andy Nunn. Underway and discrete measurements presented in this manuscript are archived at CDIAC (cdiac.ornl.gov/ftp/oceans/VOS_Gould_Lines/). Discrete observations from the Drake Passage Time-series are also archived at http://www.ldeo.columbia.edu/res/pi/CO2/carbondioxide/pages/global_ph.html. Contact david.munro@colorado.edu for data from 2015.

References

- Bates, N.R., Y.M. Astor, M.J. Church, K. Currie, J.E. Dore, M. González-Dávila, L. Lorenzoni, F. Muller-Karger, J. Olafsson, and J.M. Santana-Casiano (2014), A time-series view of changing ocean chemistry due to ocean uptake of anthropogenic CO₂ and ocean acidification, *Oceanography*, 27, 126 – 141, [doi:10.5670/oceanog.2014.16](https://doi.org/10.5670/oceanog.2014.16).
- Belkin, I.M., and A.L. Gordon (1996), Southern Ocean fronts from the Greenwich meridian to Tasmania, *J. Geophys. Res.*, 101, 3675 – 3696.
- Chipman, D.W., J. Marra, and T. Takahashi (1993), Primary production at 47°N and 20°W in the North Atlantic Ocean: A comparison between the ¹⁴C incubation method and the mixed layer carbon budget, *Deep-Sea Res. II*, 40, 151 – 169.
- Currie, K.I., M.R. Reid, and K.A. Hunter (2011), Interannual variability of carbon dioxide drawdown by subantarctic surface water near New Zealand, *Biogeochemistry* 104, 23 – 34, [doi:10.1007/s10533-009-9355-3](https://doi.org/10.1007/s10533-009-9355-3).
- Dong, S., J. Sprintall, and S.T. Gille (2006), Location of the Antarctic Polar Front from AMSR-E satellite sea surface temperature measurements, *J. Phys. Oceanogr.* 36, 2075 – 2089, [doi:10.1175/JPO2973.1](https://doi.org/10.1175/JPO2973.1).
- Egleston, E.S., C.L. Sabine, and F.M.M. Morel (2010), Revelle revisited: Buffer factors that quantify the response of ocean chemistry to changes in DIC and alkalinity, *Global Biogeochem. Cycles*, 24, GB1002, [doi:10.1029/2008GB003407](https://doi.org/10.1029/2008GB003407).
- Fabry, V.J., J.B. McClintock, J.T. Mathis, and J.M. Grebmeier (2009), Ocean acidification at high latitudes: The bellweather, *Oceanography*, 22, 160 – 171.
- Fay, A.R., and G.A. McKinley (2013), Global trends in surface ocean pCO₂ from in situ data, *Global Biogeochem. Cycles*, 27, 541 – 557, [doi:10.1002/gbc.20051](https://doi.org/10.1002/gbc.20051).
- Fay, A.R., G.A. McKinley, and N.S. Lovenduski (2014), Southern Ocean carbon trends: Sensitivity to methods, *Geophys. Res. Lett.*, 41, 6833 – 6840, [doi:10.1002/2014GL061324](https://doi.org/10.1002/2014GL061324).
- Hauck, J., and C. Völker (2015), Rising atmospheric CO₂ leads to large impact of biology on Southern Ocean CO₂ uptake via changes of the Revelle factor, *Geophys. Res. Lett.*, 42, 1459 – 1464, [doi:10.1002/2015GL063070](https://doi.org/10.1002/2015GL063070).

- Hauck, J., M. Hoppema, R.G.J. Bellerby, C. Völker, and D. Wolf-Gladrow (2010), Data-based estimation of anthropogenic carbon and acidification in the Weddell Sea on a decadal timescale, *J. Geophys. Res.*, *115*, C03004, doi:10.1029/2009JC005479.
- Khatiwala, S., F. Primeau, and T. Hall (2009), Reconstruction of the history of anthropogenic CO₂ concentrations in the ocean, *Nature*, *462*, doi:10.1038/nature08526.
- Landschützer, P., N. Gruber, D.C.E. Bakker, and U. Schuster (2014), Recent variability of the global ocean carbon sink, *Global Biogeochem. Cycles*, *28*, doi:10.1002/2014GB004853.
- Lenton, A., et al. (2013), Sea-air CO₂ fluxes in the Southern Ocean for the period 1990–2009, *Biogeosciences*, *10*, 4037 – 4054, doi:10.5194/bg-10-4037-2013.
- Lenton, A., N. Metzl, T. Takahashi, M. Kuchinke, R. J. Matear, T. Roy, S. C. Sutherland, C. Sweeney, and B. Tilbrook (2012), The observed evolution of oceanic pCO₂ and its drivers over the last two decades, *Global Biogeochem. Cycles*, *26*, GB2021, doi:10.1029/2011GB004095.
- Le Quéré, C., T. Takahashi, E.T. Buitenhuis, C. Rödenbeck, and S.C. Sutherland (2010), Impact of climate change and variability on the global oceanic sink of CO₂, *Global Biogeochem. Cycles*, *24*, GB4007, doi:10.1029/2009GB003599.
- Lovenduski, N.S., A.R. Fay, and G.A. McKinley (2015), Observing multidecadal trends in Southern Ocean CO₂ uptake: What can we learn from an ocean model?, *Global Biogeochem. Cycles*, *29*, 416-426, doi:10.1002/2014GB004933.
- Lovenduski, N.S., M.C. Long, P.R. Gent, and K. Lindsay (2013), Multi-decadal trends in the advection and mixing of natural carbon in the Southern Ocean, *Geophys. Res. Lett.*, *40*, 139 – 142, doi:10.1029/2012GL054483.
- Lovenduski, N.S., N. Gruber, S.C. Doney, and I.D. Lima (2007), Enhanced CO₂ outgassing in the Southern Ocean from a positive phase of the Southern Annular Mode, *Global Biogeochem. Cycles*, *21*, GB2026, doi:10.1029/2006GB002900.
- Lueker, T.J., A.G. Dickson, and C.D. Keeling (2000), Ocean pCO₂ calculated from dissolved inorganic carbon, alkalinity and equations K1 and K2: validation based on laboratory measurements of CO₂ in gas and seawater at equilibrium, *Mar. Chem.*, *70*, 105 – 119.

Majkut, J.D., J.L. Sarmiento, and K.B. Rodgers (2014), A growing oceanic carbon uptake: Results from an inversion study of surface pCO₂ data, *Global Biochem. Cycles*, 28, 335 – 351, doi:10.1002/2013GB004585.

Mattsdotter Björk, M., A. Fransson, A. Torstensson, and M. Chierici (2014), Ocean acidification state in western Antarctic surface waters: controls and interannual variability, *Biogeosciences*, 11, 57 – 73, doi:10.5194/bg-11-57-2014.

McNeil, B.I., and R.J. Matear (2008), Southern Ocean acidification: A tipping point at 450-ppm atmospheric CO₂, *PNAS*, 105, 18860 – 18864, doi:10.1073/pnas.0806318105.

Metzl, N. (2009), Decadal increase of oceanic carbon dioxide in Southern Indian Ocean surface waters (1991–2007), *Deep-Sea Res. II*, 56, 607 – 619, doi:10.1016/j.dsr2.2008.12.007

Munro, D.R. et al. (2015), Estimates of net community production in the Southern Ocean determined from time series observations (2002 – 2011) of nutrients, dissolved inorganic carbon, and surface ocean pCO₂ in Drake Passage, *Deep-Sea Res. II*, 114, 49 – 63, doi:10.1016/j.dsr2.2014.12.014.

Pardo, P.C., F.F. Pérez, S. Khatiwala, and A.F. Ríos (2014), Anthropogenic CO₂ estimates in the Southern Ocean: Storage partitioning in the different water masses, *Prog. Oceanogr.*, 120, 230 – 242, doi:10.1016/j.pocean.2013.09.005.

Riebesell, U., A. Körtzinger, and A. Oschlies (2009), Sensitivities of marine carbon fluxes to ocean change, *Proc. Natl. Acad. Sci. U.S.A.*, 106(49), 20,602 – 20,609, doi:10.1073/pnas.0813291106.

Roden, N.R., E.H. Shadwick, B. Tilbrook, and T.W. Trull (2013), Annual cycle of carbonate chemistry and decadal acidification change in coastal Prydz Bay, East Antarctica, *Mar. Chem.*, 155, 135 – 147, doi: 10.1016/j.marchem.2013.06.006.

Shadwick, E.H., T.W. Trull, B. Tilbrook, A.J. Sutton, E. Schulz, and C.L. Sabine (2015), Seasonality of biological and physical controls on surface ocean CO₂ from hourly observations at the Southern Ocean Time Series site south of Australia, *Global Biogeochem. Cycles*, 29, 223 – 238, doi:10.1002/2014GB004906.

Shadwick, E.H., T.W. Trull, H. Thomas, and J.A.E. Gibson (2013), Vulnerability of Polar oceans to anthropogenic acidification: An Arctic-Antarctic comparison, *Nat. Sci. Rep.*, 3, 2339, doi: 10.1038/srep02339.

Stephenson, G.R., Jr., S.T. Gille, and J. Sprintall (2012), Seasonal variability of upper ocean heat content in Drake Passage, *J. Geophys. Res.*, *117*, C04019, doi:10.1029/2011JC007772.

Sweeney, C., E. Gloor, A.R. Jacobson, R.M. Key, G. McKinley, J.L. Sarmiento, and R. Wanninkhof (2007), Constraining global air-sea gas exchange for CO₂ with recent bomb ¹⁴C measurements, *Global Biogeochem. Cycles*, *21*, GB2015, doi:10.1029/2006GB002784.

Takahashi, T., S.C. Sutherland, D.W. Chipman, J.G. Goddard, C. Ho, T. Newberger, C. Sweeney, and D.R. Munro (2014), Climatological distributions of pH, pCO₂, total CO₂, alkalinity, and CaCO₃ saturation in the global surface ocean, and temporal changes at selected locations, *Mar. Chem.*, *164*, 95 – 125. doi: 10.1016/j.marchem.2014.06.004.

Takahashi, T., C. Sweeney, B. Hales, D.W. Chipman, T. Newberger, J.G. Goddard, R.A. Iannuzzi, and S.C. Sutherland (2012), The changing carbon cycle in the Southern Ocean, *Oceanography*, *25*, 26 – 37.

Takahashi, T., R.A. Feely, R.F. Weiss, R.H. Wanninkhof, D.W. Chipman, S.C. Sutherland, and T.T. Takahashi (1997), Global air-sea flux of CO₂: An estimate based on measurements of sea-air pCO₂ difference, *Proc. Natl. Acad. Sci.*, *94*, 8292 – 8299.

Takahashi, T., J. Olafsson, J. Goddard, D.W. Chipman, and S.C. Sutherland (1993), Seasonal variation of CO₂ and nutrients in the high-latitude surface oceans: A comparative study, *Global Biogeochem. Cycles*, *7*, 843 – 878.

van Heuven, S.M.A.C., M. Hoppema, E.M. Jones, and H.J.W. de Baar (2014), Rapid invasion of anthropogenic CO₂ into the deep circulation of the Weddell Gyre, *Philos. T. Roy. Soc. A*, *372*, 20130056, doi:10.1098/rsta.2013.0056.

Wanninkhof, R., G.-H. Park, T. Takahashi, C. Sweeney, R. Feely, Y. Nojiri, N. Gruber, S.C. Doney, G.A. McKinley, A. Lenton, C. Le Quéré, C. Heinze, J. Schwinger, H. Graven, and S. Khatiwala, (2013), Global ocean carbon uptake: magnitude, variability and trends, *Biogeosciences*, *10*, 1983 – 2000, doi:10.5194/bg-10-1983-2013.

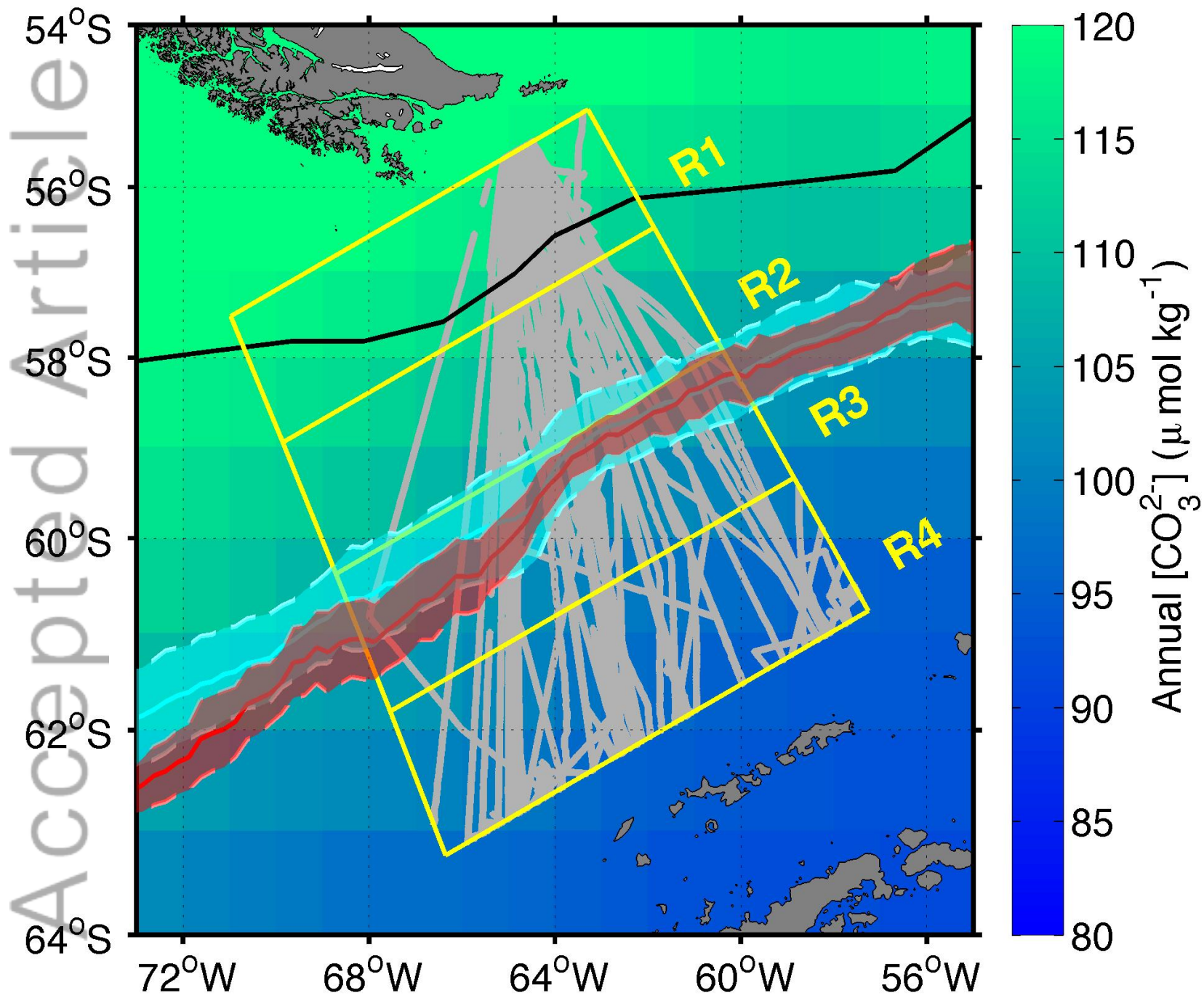
Figure Captions

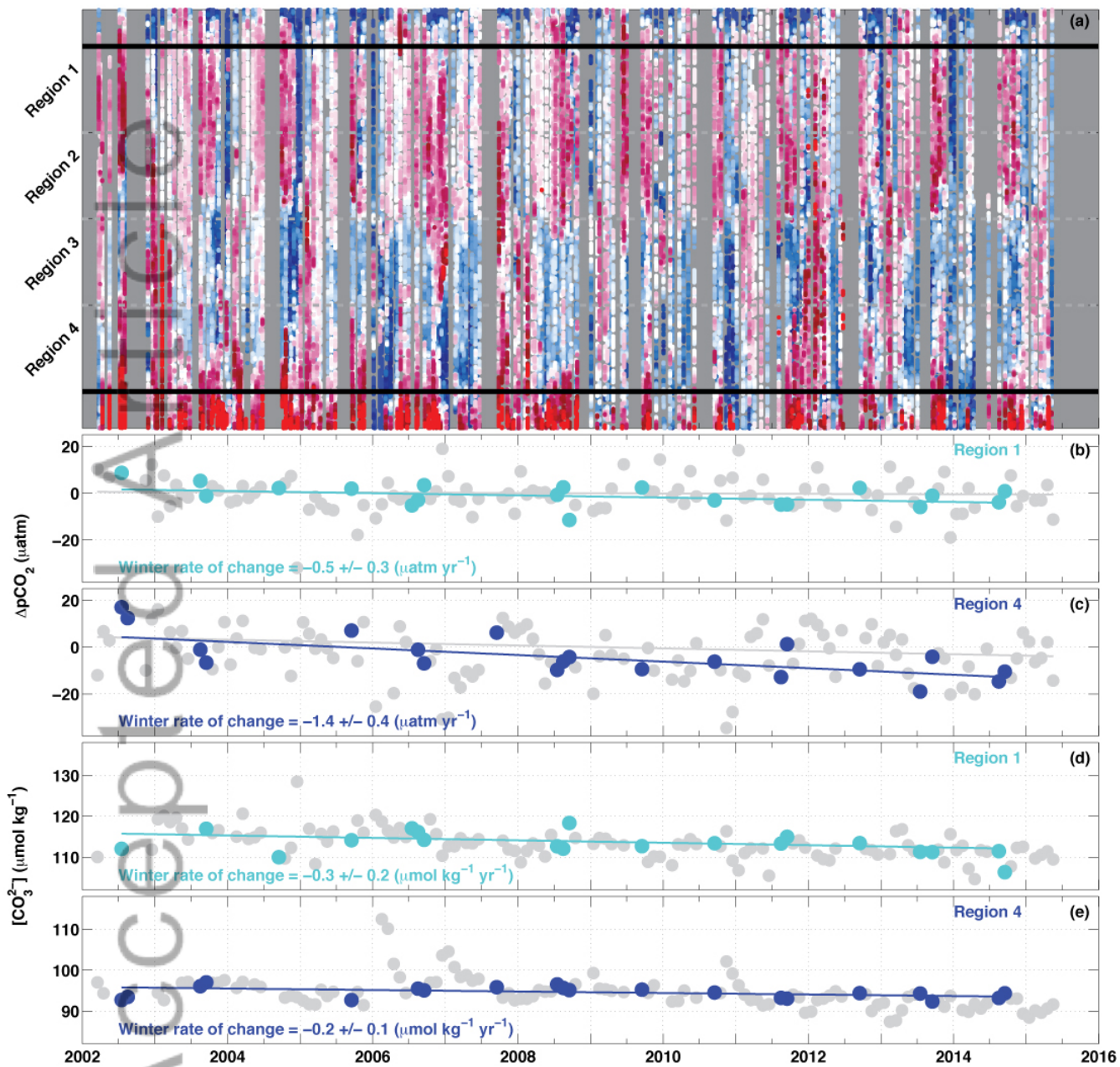
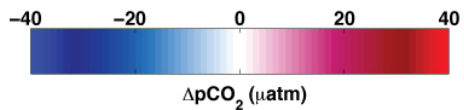
Figure 1. Drake Passage regions used in this study. The divisions are identical to those used by Munro et al. (2015). Gray lines indicate cruise tracks with underway $p\text{CO}_{2\text{surf}}$ data through any of the four regions from 2002-2015. The black line indicates the mean position of the Subantarctic Front (SAF) as determined by Belkin and Gordon (1996). For the APF, both summer (red line) and winter (blue line) positions are shown with shading indicating the standard deviation of the APF position in each season from 2002-2011. APF positions were determined using AMSR-E SST data using a procedure similar to Dong et al. (2006). Cruise tracks are overlain on annual $[\text{CO}_3^{2-}]$ calculated using the climatology of Takahashi et al. (2014).

Figure 2. Time-series of all $\Delta p\text{CO}_2$ observations from 2002-2015 (a) and monthly regional averages for $\Delta p\text{CO}_2$ (panels (b) and (c)) and $[\text{CO}_3^{2-}]$ (panels (d) and (e)) for DPT Regions 1 and 4. Winter (i.e., July through September) observations and time-series trends are indicated in blue and observations for all other months and the time-series trend based on all available data are indicated in gray for panels (b) through (e). The seasonal cycle based on monthly time-series means was removed prior to calculation of the trends shown in panels (b)-(e); the time-series mean was then added back to the monthly anomalies to produce the deseasonalized time-series plotted here.

Figure 3. Growth rates in $p\text{CO}_2$ and contributions to $p\text{CO}_{2\text{surf}}$ for all months, summer, and winter and associated uncertainties (i.e., 1σ standard error of the trends) averaged over all four regions of the DPT (i.e., Regions 1-4) for the period 2002-2015. Both atmospheric (ATM) and oceanic (OCE) growth rates are included in addition to the four drivers of ocean $p\text{CO}_{2\text{surf}}$: sea surface temperature (SST), sea surface salinity (SSS), total alkalinity (TA), and total CO_2 (TCO_2). The growth rate in $p\text{CO}_{2\text{surf}}$ due to TCO_2 changes is further separated into salinity-normalized ($s\text{TCO}_2$) and salinity-driven (fwTCO_2) components following Lovenduski et al. (2007).

ACCEPTED MANUSCRIPT





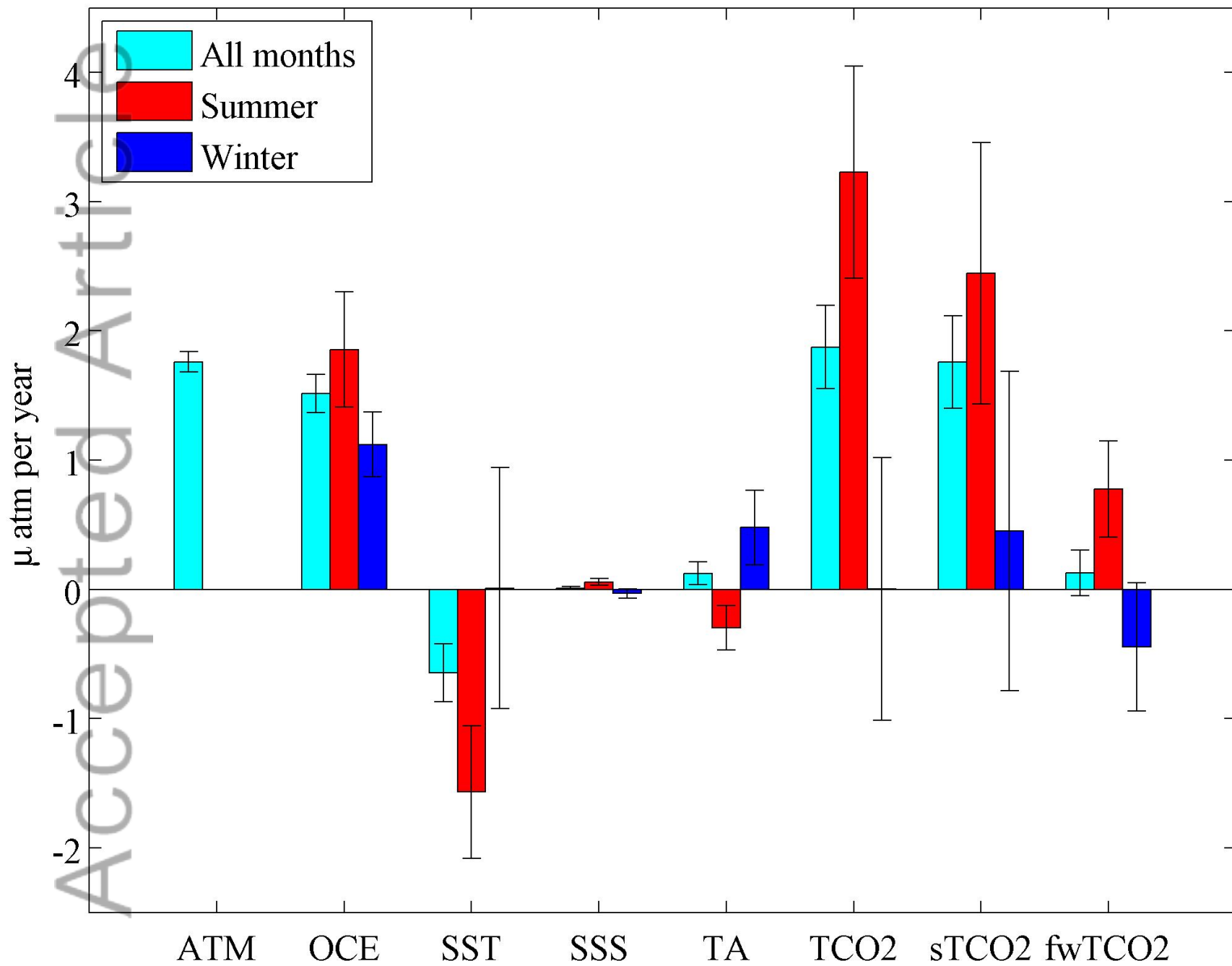


Table 1. Mean annual, summer (December through February), and winter (July through September) rates of change in $\Delta p\text{CO}_2$ and $[\text{CO}_3^{2-}]$ for the Drake Passage with regions as shown in Fig. 1. The regions are numbered in north to south order. Uncertainties in rates of change are given by the standard error of the trend. Significant trends, with non-overlapping 1-sigma values, are indicated in bold.

	Annual $\Delta p\text{CO}_2$ $\mu\text{atm yr}^{-1}$	Summer $\Delta p\text{CO}_2$ $\mu\text{atm yr}^{-1}$	Winter $\Delta p\text{CO}_2$ $\mu\text{atm yr}^{-1}$	Annual $[\text{CO}_3^{2-}]$ $\mu\text{mol kg}^{-1} \text{yr}^{-1}$	Summer $[\text{CO}_3^{2-}]$ $\mu\text{mol kg}^{-1} \text{yr}^{-1}$	Winter $[\text{CO}_3^{2-}]$ $\mu\text{mol kg}^{-1} \text{yr}^{-1}$
Region 1	-0.09±0.17	+0.43±0.59	-0.47±0.28	-0.52±0.07	-0.75±0.21	-0.30±0.16
Region 4	-0.62±0.27	-0.51±0.84	-1.40±0.41	-0.45±0.08	-0.70±0.26	-0.18±0.08
Drake Passage (all 4 regions)	-0.37±0.16	-0.03±0.47	-1.03±0.30	-0.57±0.08	-0.83±0.22	-0.14±0.23

Accepted Article